The role of alkali cations in zeolite synthesis from silicate solutions containing N,N,N-trimethyl-1-adamantammonium cations

C.S. Gittleman, A.T. Bell and C.J. Radke

Center for Advanced Materials, Materials Sciences Division, Lawrence Berkeley National Laboratory, and Department of Chemical Engineering, University of California, Berkeley, CA 94720, USA

Received 31 August 1995; accepted 6 December 1995

Zeolite synthesis from aqueous N,N,N-trimethyl-1-adamantammonium ($TMAA^+$)–alkali (Na^+, K^+, Rb^+, and Cs^+) silicate mixtures is studied using X-ray diffraction, elemental analysis, scanning electron microscopy, and ^{29}Si magic angle spinning (MAS), ^1H–^{13}C cross-polarization (CP) MAS and ^1H–^{29}Si CP MAS NMR spectroscopies. SSZ-24 forms in the presence of potassium cations, and SSZ-31 crystallizes in the presence of sodium cations. This is the first report of SSZ-31 synthesis from Na–TMAA silicate mixtures. Unknown silicates form in the presence of rubidium and cesium cations, whereas no crystalline material is observed in synthesis mixtures devoid of alkali cations. The alkali cations do not appear to serve as templates or void fillers during zeolite crystallization, nor do they stabilize soluble silicate anions which serve as building blocks during zeolite crystallization. Rather, the alkali cations appear to regulate the transformation of the amorphous synthesis gel into either crystalline zeolite or other silicate phases.

Keywords: zeolite synthesis; SSZ-24; SSZ-31; alkali cations; N,N,N-1-adamantammonium cation

1. Introduction

Purely siliceous zeolites are typically synthesized by hydrothermal treatment of silicate gels containing organic and alkali cations. A number of recent studies have elucidated the structure-directing or "templating" role of the organic during the synthesis of Al-free zeolites [1–6]. However, much less is known about the role(s) of alkali cations in directing the progress of zeolite formation. Inorganic cations are known to affect the crystallinity, yield, crystal morphology, and rate of formation of synthetic zeolites [7]. In high silica synthesis mixtures ($Si/Al > 85$) containing alkali cations and hexane-1,6-diamine, ZSM-5 forms when Li^+ cations are used, and Nu-10 of varying purity forms in synthesis mixtures containing Na^+ (85% crystallinity), K^+ (100% crystallinity), Rb^+ (90% crystallinity), and Cs^+ (65% crystallinity) cations [8]. Additionally, the time to nucleate Nu-10 increases with increasing size of the alkali cation [8]. In ZSM-5 synthesis mixtures containing tetrapropylammonium (TPA^+) and NH_4^+ cations, twinned crystals smaller than 10 μm form [9]. The addition of Na_2O and K_2O promotes the formation of 20 and 26 μm ZSM-5 crystals, respectively, while the addition of Li^+ cations promotes the formation of lathe-shaped ZSM-5 crystals over 100 μm in length [9]. Finally, Erdem and Sand showed that ZSM-5, mordenite, harmotome, or analcime can form from aluminosilicate mixtures containing alkali and TPA^+ cations ($Si/Al = 28$), depending on the relative amounts of Na^+ and K^+ in the synthesis mixture [10].

Silicalite-1 can be synthesized from aluminosilicate gels containing tetraalkylammonium (TAA^+) and alkali cations, where Li^+, Na^+, K^+, Rb^+, and Cs^+ cations have all been used in silicalite synthesis [11,12], but, silicalite can also be synthesized in the absence of metal cations [2]. On the other hand, pure SSZ-24 has only been synthesized from silicate mixtures containing potassium and N,N,N-trimethyl-1-adamantammonium ($TMAA^+$) cations [13,14]. This zeolite can, however, be made together with an impurity layered silicate using N-methyl sparteine cations [15].

The present study investigates zeolite synthesis from $TMAA^+$-silicate mixtures containing various alkali cations (alkali = Na^+, K^+, Rb^+, and Cs^+). The purpose of this study is to identify the role of alkali cations during SSZ-24 synthesis. Attention is focussed on the effect of the alkali cation on the chemistry of the zeolite synthesis gel, and on the structure of the zeolite products. The synthesis gels are analyzed by X-ray diffraction (XRD), elemental analysis, scanning electron microscopy (SEM), ^{29}Si magic angle spinning (MAS), ^1H–^{13}C cross-polarization (CP) MAS and ^1H–^{29}Si CP MAS nuclear magnetic resonance (NMR) spectroscopies.

2. Experimental

2.1. Synthesis

Zeolite synthesis mixtures were prepared by the following procedure. First, an aqueous solution of AOH (98%, Fisher) and TMAAOH is prepared, where A is an alkali metal (A = Na, K, Rb, or Cs). The organic base

is formed by mixing a 1.25 M aqueous solution of TMAAI (provided by Chevron Research and Technology) with AG 1-X8 anion exchange resin (Bio-Rad) for 24 h at room temperature (H_2O/resin = 1/2 by volume.) TMAAOH concentration is determined by titration with aqueous 0.1 N HCl (Fisher). Fumed silica (Cab-O-Sil, grade EH-5) is then added to the aqueous solution, forming a mixture with a composition of 0.075 $TMAA_2O$, 0.05 A_2O, SiO_2, 44 H_2O. The mixture is stirred at room temperature for 2 h to ensure complete dissolution of the silica, thus forming a cloudy liquid with a pH of approximately 11.4. Additionally, a synthesis mixture was prepared without any alkali hydroxide. The preparation conditions for all synthesis mixtures are listed in table 1.

Immediately after preparation, each synthesis mixture was placed into 23 cm^3 static, teflon (PTFE)-lined, stainless steel autoclaves, and heated in an oven at 150°C. Following a specified period of heating, the autoclave was removed from the oven and immediately placed in an ice water bath to quench the synthesis process. The synthesis mixture was then centrifuged (2500 rpm) to separate the solid/gel phase from the mother liquor. The solids were washed with deionized water and portions were dried at 95°C to be analyzed by XRD and SEM. A portion of the unheated initial synthesis mixture was also centrifuged, washed, and dried for analysis. The mother liquor was analyzed to determine its pH and elemental composition.

2.2. Analytical procedures

The solid and liquid phases of the synthesis gels were analyzed for chemical composition. C and N contents were determined by combustion analysis, and Si and alkali contents were determined by inductively coupled plasma (ICP) emission spectroscopy. Samples were prepared for ICP analysis by dissolving the solids in an acid mixture with volumetric composition 0.9HF : 2.1HCl : HNO_3 : $15H_3BO_3$(5%) : $31H_2O$[16].

X-ray powder patterns were obtained on a Siemens Kristalloflex diffractometer with Cu Kα radiation. Samples were step-scanned for 2θ values from 5 to 40°, using 0.05° steps and 2 s counts. The size and morphology of the solids were characterized by SEM, using an ISI-DS130 dual stage electron microscope. Prior to examination, samples were mounted with carbon paste on aluminum pegs and coated with a film of evaporated gold.

All NMR experiments were performed on a 400 MHz Nalorac spectrometer equipped with a Doty MAS probe. Wet solids were spun at 3 kHz in sealed zirconia rotors, as described by Ginter et al. [17]. Room-temperature ^{29}Si MAS NMR spectra were obtained by signal averaging 1024 90° pulses at a resonance frequency of 79.324 MHz and an 8 s recycle delay. ^{29}Si NMR spectra are referenced to tetramethylsilane (TMS) (0 ppm). For the CP MAS NMR studies, a CP pulse sequence was used as originally described by Torchia [18]. For the ^1H–^{29}Si CP MAS spectra with ^1H decoupling, 1024 scans were taken at a resonance frequency of 79.324 MHz, with a 4 s recycle time and CP contact times ranging from 1–8 ms. For the ^1H–^{13}C CP MAS spectra with ^1H decoupling, 1024 scans were taken at a resonance frequency of 100.415 MHz, with a 2 s recycle time and a CP contact time of 2 ms. ^{13}C NMR spectra are referenced to the methylene peak of adamantane (38.4 ppm downfield from TMS). Exponential line broadening of 40 Hz was applied to all NMR data. Peak intensities were determined by fitting a lorentzian to each NMR peak.

Table 1
Synthesis parameters and results

Synthesis mixture	Alkali	Products	Nucleation time[a] (d)	Plateau time[b] (d)
1	Na	SSZ-31	15	27
2	K	SSZ-24	6	12
3	Rb	unknown silicate	12	–
4	Cs	unknown silicate	6	–
5	none	amorphous	–	–

[a] Time when crystalline material is first observed by XRD.
[b] Time when zeolite XRD peaks reach their maximum intensity.

3. Results

Figs. 1–4 show series of XRD patterns of the solids obtained from synthesis mixtures prepared with the different alkali cations. In all syntheses there is an induction period prior to the observation of crystalline material. SSZ-24 only forms from the synthesis mixture prepared with KOH. As previously reported, crystalline SSZ-24 is first evident in the XRD patterns in fig. 2 after 6 days at 150°C, and the SSZ-24 XRD peaks reach their maximum intensities after 12 days [19]. When NaOH is used in the preparation of the synthesis mixture, XRD peaks are first observed in fig. 1 between 15 and 21 days at 150°C, and by 24 days the XRD pattern is identifiable as that of SSZ-31 [20]. The SSZ-31 peaks continue to grow until 27 days. This is the first report of SSZ-31 synthesis from a silicate mixture containing $TMAA^+$ and Na^+ cations. While the exact crystal structure of SSZ-31 is not known, this zeolite, like SSZ-24, has a one-dimensional pore system with large, 12-Si atom ring channels [20]. No zeolite phases form in synthesis mixtures prepared with RbOH or CsOH. In the Rb^+ system, an unidentified silicate forms after heating for 12 to 15 days at 150°C (fig. 3). In the Cs^+ system, an unidentified silicate forms after 4 to 8 days of heating at 150°C (fig. 4). The XRD pattern in fig. 4 changes as the synthesis mixture is heated between 8 and 15 days, indicating that there is a change in the structure of the silicate after its initial crystallization. No crystalline material forms in the synthesis gel prepared without alkali cations. The synthesis results of all synthesis mixtures are summarized in table 1.

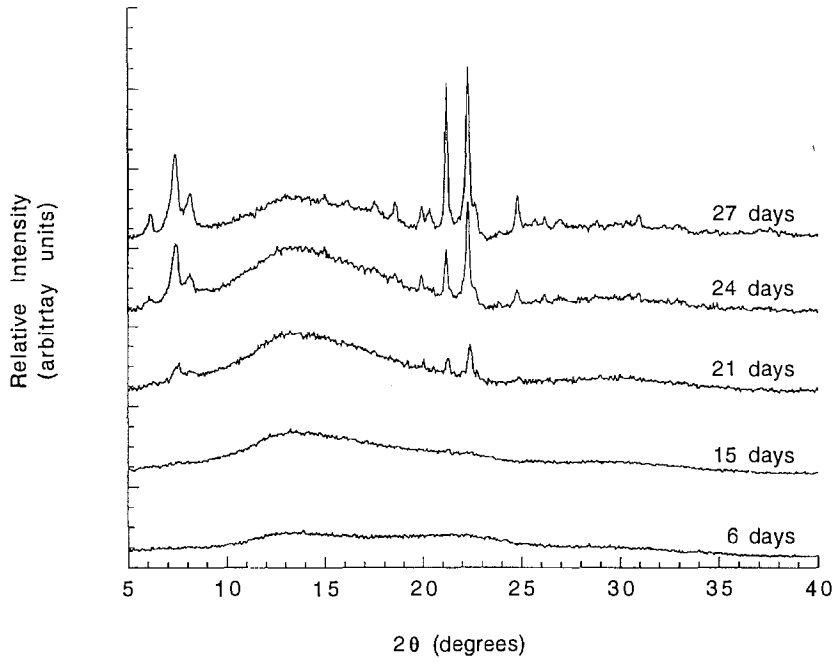

Fig. 1. Powder X-ray diffraction patterns of dried solids obtained from a Na–TMAA synthesis mixture heated at 150°C for various times.

Scanning electron micrographs of the solids obtained from synthesis gels prepared using the various alkali cations are shown in fig. 5. As previously reported [19], 25 × 15 μm hexagonal prism SSZ-24 crystals form in the gel prepared using KOH, similar to those observed by Van Nordstrand et al. [13] (fig. 5b). In the Na^+ system, 20 μm wide fan-shaped SSZ-31 crystals form (fig. 5a). Similar SSZ-31 crystals were observed by Nakagawa and Zones when using an organic template based on an aza-tricycloundecane [21]. Cauliflower-type crystals of an unidentified silicate form in the Rb^+-containing synthesis gels (fig. 5c), and irregular, non-uniform crystals of an unknown silicate form in synthesis gels prepared with CsOH (fig. 5d).

The ratios of Si per $TMAA^+$ cations in the solids obtained from Na^+- and K^+-containing synthesis mixtures are plotted as functions of heating time in fig. 6. In the K^+ system, the Si/TMAA ratio in the solids increases steadily during the induction period, and then decreases rapidly to Si/TMAA = 26 during crystal growth (fig. 6b) [19]. Similar behavior is observed in the Na^+ system during SSZ-31 synthesis. The sum of the XRD peak intensities of the SSZ-31 peaks at $2\theta = 21.2$ and 22.3° and the Si/TMAA ratio in the solids obtained

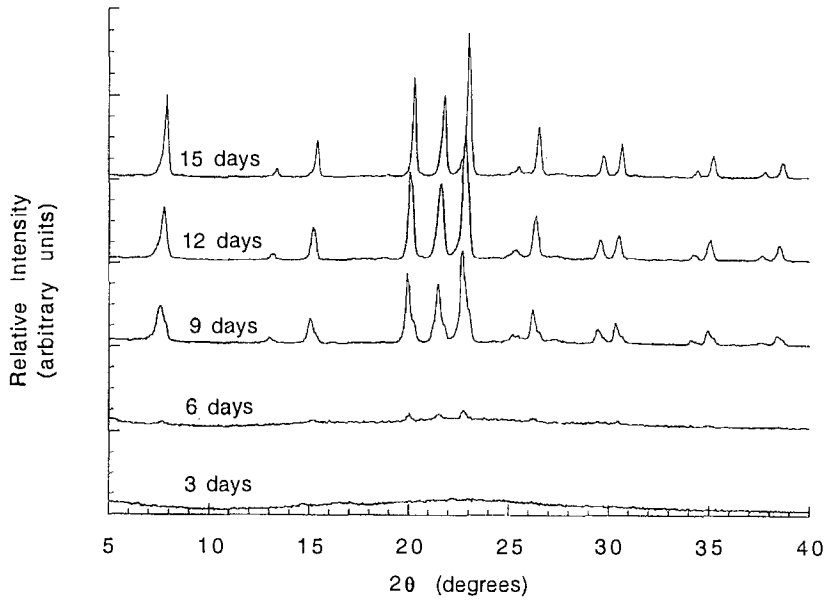

Fig. 2. Powder X-ray diffraction patterns of dried solids obtained from a K–TMAA synthesis mixture heated at 150°C for various times.

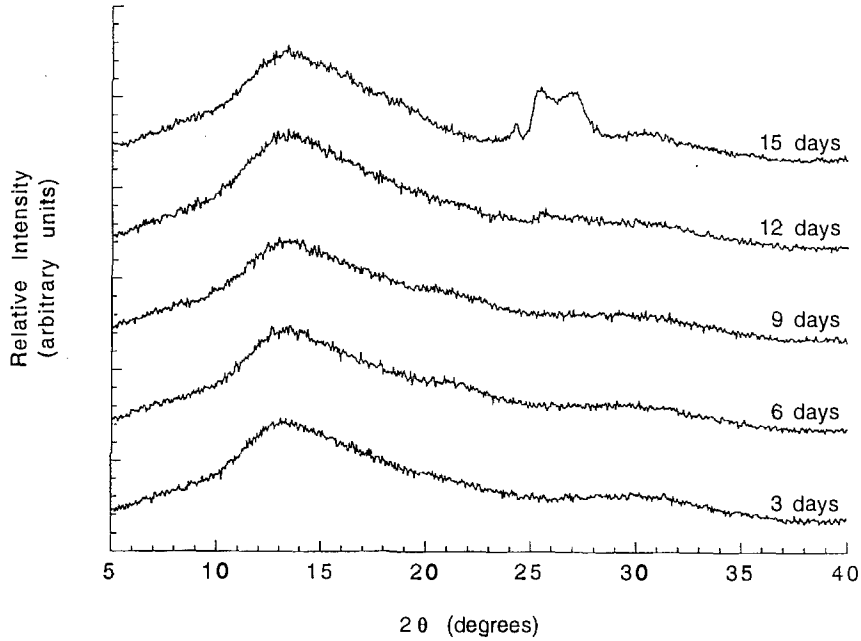

Fig. 3. Powder X-ray diffraction patterns of dried solids obtained from a Rb–TMAA synthesis mixture heated at 150°C for various times.

from synthesis gels prepared using NaOH as functions of heating time are shown in fig. 6a. The Si/TMAA ratio rises during the induction period, and reaches a maximum after 15 days at 150°C, corresponding to the time when crystalline material is first observed by XRD (fig. 1). The Si/TMAA ratio then decreases during crystal growth, until levelling off at Si/TMAA = 30 when the SSZ-31 XRD peaks reach their maximum intensities. The rates of both the increase and subsequent decrease of the Si/TMAA ratio in the solids are slower in the Na^+ system than in the K^+ system. In both the Rb^+ and Cs^+ systems the Si/TMAA ratio remains between 30 and 40 throughout the synthesis.

In the K^+ system, one K^+ cation is incorporated into the SSZ-24 lattice per 110 Si atoms [19]. By contrast, no alkali cations are incorporated into solid products obtained from synthesis mixtures prepared with Na^+, Rb^+, or Cs^+ cations. The elemental analysis results of the crystalline products obtained from all syntheses are summarized in table 2.

In both the Na^+- and K^+-containing synthesis mixtures, the pH of the mother liquor is about 11.6 during

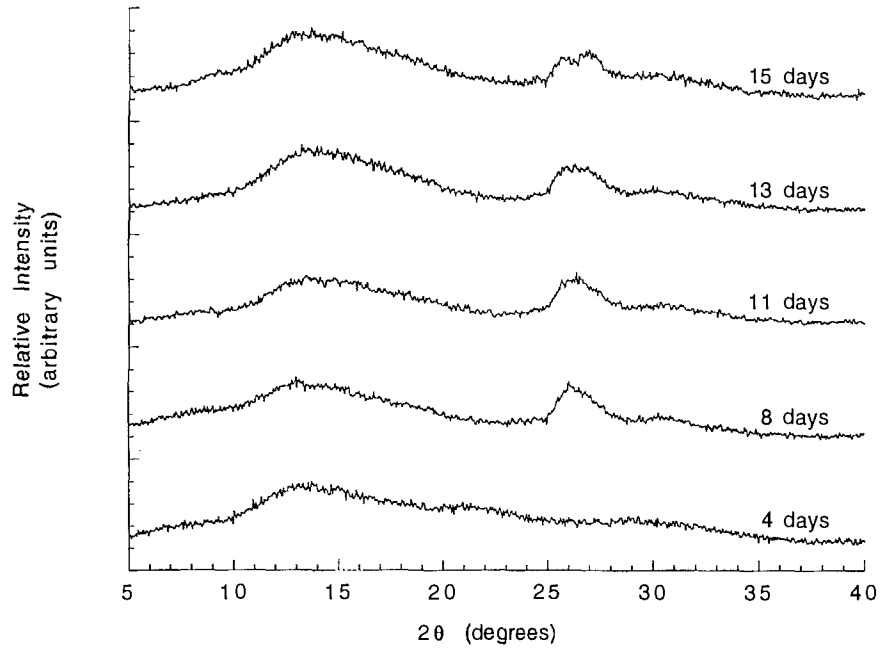

Fig. 4. Powder X-ray diffraction patterns of dried solids obtained from a Cs–TMAA synthesis mixture heated at 150°C for various times.

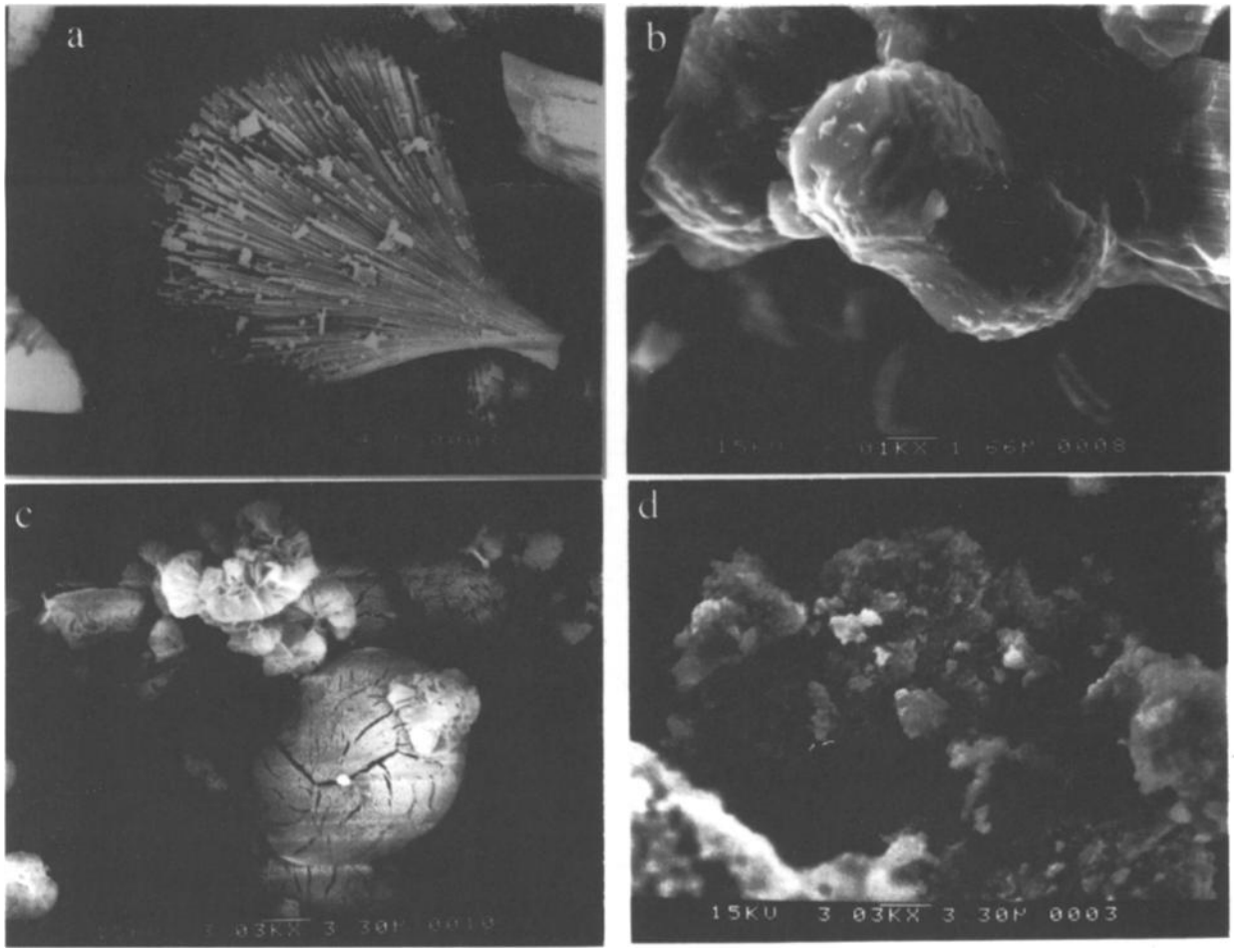

Fig. 5. Scanning electron micrographs of (a) SSZ-31 crystals obtained from a Na–TMAA synthesis mixture; (b) SSZ-24 crystals obtained from a K–TMAA synthesis mixture; (c) unidentified silicate crystals obtained from a Rb–TMAA synthesis mixture; (d) unknown silicate obtained from a Cs–TMAA synthesis mixture. Horizontal white markers below micrographs indicate the length scale.

the induction period. As previously reported [19], the pH of the mother liquor in the K^+ system rises rapidly to 12.0 during SSZ-24 crystal growth. Similar results are observed in the Na^+ system, as the pH of the mother liquor rises rapidly to 11.92 during SSZ-31 crystallization.

^1H–^{29}Si CP MAS NMR is used to probe the interactions between the $TMAA^+$ protons and the silica in the solids obtained from the Na^+-containing synthesis mixtures from which SSZ-31 crystallizes. The details of the analysis procedures are described elsewhere [19]. Fig. 7a shows a series of ^{29}Si MAS NMR spectra without CP of the solids obtained from Na-TMAA-synthesis mixtures after increasing heating times. The Q^3 peaks (between -100 and -105 ppm) and Q^4 peaks (between -110 and -115 ppm) correspond to Si atoms connected via siloxane bonds to three other Si atoms and to four other Si atoms, respectively. The signal to noise ratio of the spectra without CP in fig. 7a is too poor to get accurate peak areas. Nonetheless, a substantial decrease in the ratio of Q^3 to Q^4 peak intensity is observed between 21 and 27 days. The time between 21 and 27 days of heating corresponds to the period of SSZ-31 crystal growth (fig. 1). However, no substantial change in the Q^3/Q^4 ratio is observed prior to 21 days at 150°C.

Fig. 7b shows a series of ^1H–^{29}Si CP MAS NMR spectra of the same samples as used in fig. 7a. All CP spectra were obtained using an 8 ms CP contact time. The intensity scales of figs. 7a and 7b are the same. After 6 days at 150°C, there is little enhancement of the NMR intensity of the spectrum taken without CP. After 15 days, when crystalline material is first observed by XRD (fig. 1), there is some enhancement of the NMR signal due to ^1H–^{29}Si cross-polarization. The NMR intensity continues to increase as SSZ-31 continues to crystallize in the gel. Similar results are reported during SSZ-24 crystallization in the K-TMAA synthesis mixtures [19]. Enhancement of the NMR signal due to ^1H–^{29}Si cross-polarization is attributed to $TMAA^+$ protons which are within close contact of the Si atoms in the solids (Si–H $\leqslant$ 3.3 Å) [5,19,22].

Fig. 8 shows a series of ^1H–^{13}C CP MAS NMR spectra of the Na^+-containing synthesis mixture after various heating times, as well as a spectrum of solid

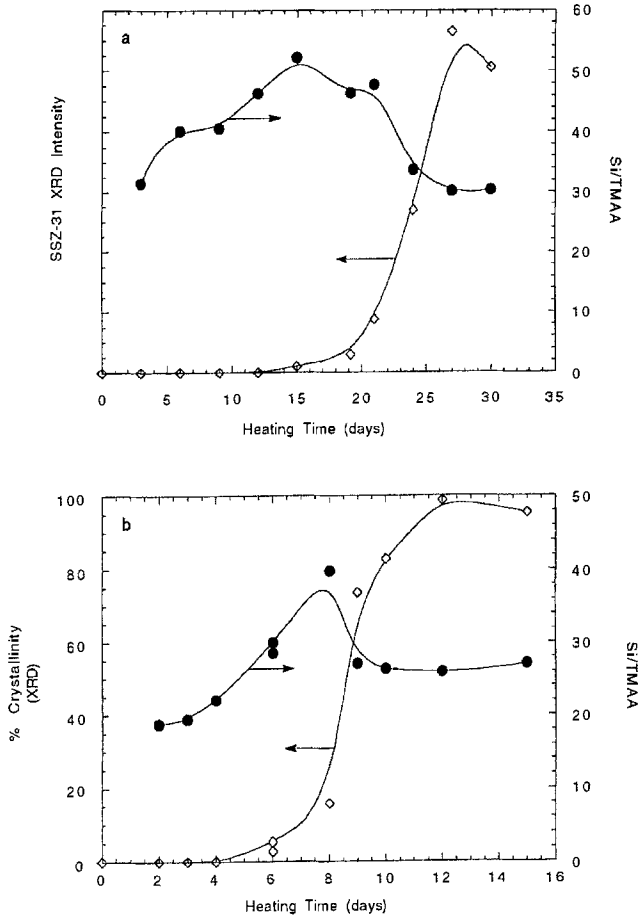

Fig. 6. (a) The sum of the XRD peak intensities of the SSZ-31 peaks at $2\theta = 21.2$ and 22.3° and the Si/TMAA ratio in the solids obtained from Na–TMAA synthesis gels and (b) the percent crystallinity of SSZ-24 and the Si/TMAA ratio in the solids obtained from K–TMAA synthesis gels as functions of heating time at 150°C.

TMAAI. Peak assignments of the carbon atoms of $TMAA^+$ are shown to the left of the spectra. All of the peaks for $TMAA^+$ incorporated into the silicate gel exhibit changes in resonance frequency and peak width compared to the peaks seen in the spectrum of TMAAI. However, the similarity between the spectra for the iodide salt and the synthesis gels indicate that $TMAA^+$ is incorporated intact into the SSZ-31 lattice. Note that the peak for the quaternary carbon atom (peak b) is very weak in the spectra of the synthesis gel because it not bonded to any protons through which cross-polarization can occur. The differences in the peak frequencies in the spectrum of the iodide salt and those of the synthesis gel suggest the chemical environment of $TMAA^+$ in TMAAI is different from that within the amorphous silicate gel. Increased peak widths of the peaks of the synthesis gel suggest either sample inhomogeneity [23] or a decreased mobility of the individual ^{13}C atoms [24] in the solids obtained from the synthesis gel. There are also several changes in the ^1H–^{13}C CP MAS NMR spectra in fig. 8 between 21 and 27 days of heating, which coincides with the increase in the crystallinity of SSZ-31 (fig. 1). In particular, the methyl peak (peak a) and the methine peak (peak d) are shifted slightly upfield as SSZ-31 crystal growth occurs. The increase in the NMR intensity between 21 and 27 days is due to the reincorporation of $TMAA^+$ cations into the solids during that time (fig. 6a).

Table 2
Summary of elemental analysis results

Synthesis mixture	Alkali	Products	Final Si/TMAA	Final Si/A [a]
1	Na	SSZ-31	30	∞
2	K	SSZ-24	26	110
3	Rb	unknown silicate	40	∞
4	Cs	unknown silicate	40	∞

[a] A = alkali cation.

The ^1H–^{13}C CP MAS NMR spectra of $TMAA^+$ cations existing in the amorphous gels obtained from Na^+- (fig. 8) and K^+-containing synthesis mixtures during the induction periods are very similar. This indicates that the structure of $TMAA^+$ cations within Na^+- and K^+-containing synthesis gels is the same. Fig. 9 compares the ^1H–^{13}C CP MAS NMR spectra of $TMAA^+$ within the fully crystalline SSZ-24 [19] and SSZ-31 lattices. The spectra for both zeolites are nearly identical, suggesting that $TMAA^+$ cations exist in similar configurations and chemical environments within the SSZ-24 and SSZ-31 channels.

4. Discussion

It is evident that alkali cations strongly affect the structure of crystalline products formed from a siliceous synthesis mixture containing $TMAA^+$ cations. Since few, if any of the alkali cations are incorporated into the crystalline products, it seems unlikely that the alkali cations play a structure-directing role similar to that of the $TMAA^+$ cation [19]. Furthermore, even though the type and concentration of alkali cations affect the distribution of soluble silicate species in aqueous silicate solutions [25,26], and soluble silicate anions, such as double-ring silicate species, may act as secondary building units (SBU's) or building blocks for zeolite formation [27], it does not appear that the primary role of the alkali cations is to stabilize SBU's in the synthesis mixtures. For example, the SSZ-24 structure, as synthesized from the K-TMAA synthesis mixture, is made up entirely of four- and six-membered ring silicate units [13]. However, when TMAAOH is replaced by TPAOH, silicalite-1 crystallizes from the K-TPA synthesis mixture [19], and the silicalite-1 lattice is made up of primarily five-membered ring silicate units [28]. Since zeolites comprised of different secondary building units form from synthesis mixtures containing the same alkali metal, it is unlikely that the main role of the alkali cation is to stabilize soluble silicate anions in aqueous solutions.

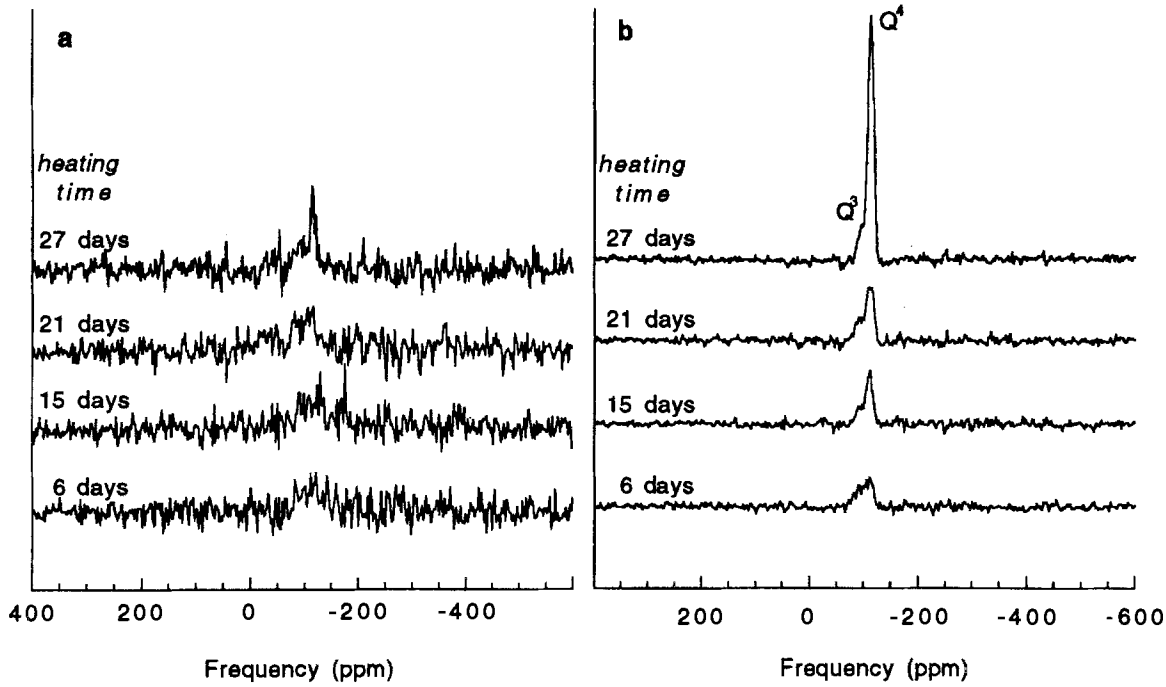

Fig. 7. (a) ^{29}Si MAS NMR spectra and (b) ^{1}H–^{29}Si CP MAS NMR spectra of solids obtained from Na–TMAA synthesis gels after various heating times at 150°C. 8 ms CP contact times were used in the CP experiments. The intensity scales of both sets of spectra are the same.

It is, therefore, more likely that the alkali cations mediate in some manner the transformation of the amorphous silicate gel into crystalline material. One possible effect of the alkali cations is to influence the rate of silica dissolution, and, hence, the concentration and the degree of polymerization of silicate anions in solutions. Additionally, the alkali cations may affect the structure of the silicate gel, and, hence, influence the facility of the amorphous gel to transform into crystalline zeolites. For example, Depasse and Watillon [29] have shown that Na^+ serves as a bridging agent to connect silica particles into a dense gel, whereas the larger K^+, Rb^+, and Cs^+ cations form double layers around the silica particles, thus hindering aggregation. Furthermore, Iler has shown that in basic solutions (pH > 10) Na^+ will flocculate silica whereas K^+ will not [30]. Such effects could explain the much slower rate of SSZ-31 formation from Na^+-containing synthesis mixtures relative to SSZ-24 formation from K^+-containing synthesis mixtures. The reason why Rb^+ and Cs^+ cations direct the synthesis

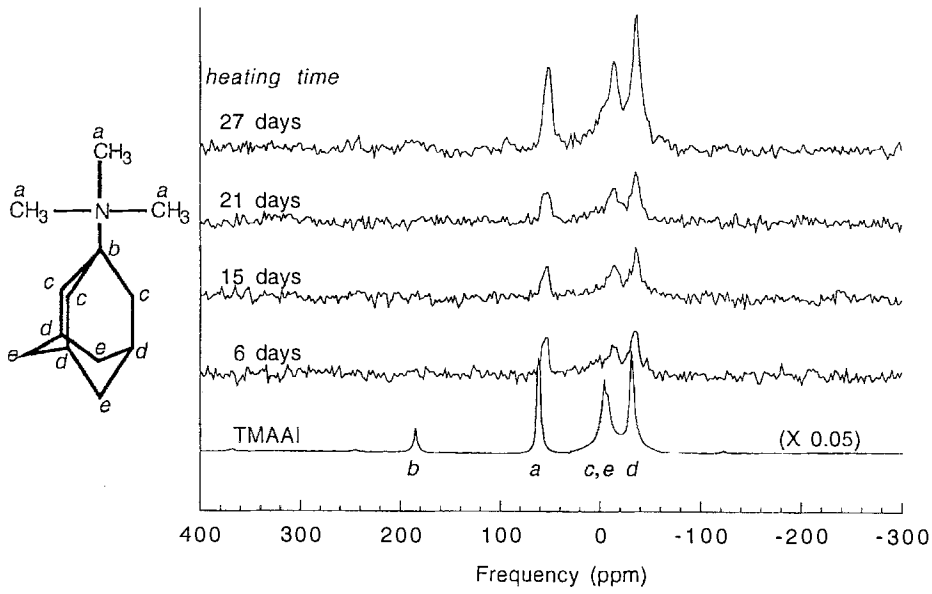

Fig. 8. ^{1}H–^{13}C CP MAS NMR spectra of solids obtained from Na–TMAA synthesis mixtures after various heating times at 150°C. The bottommost spectrum is of a TMAAI salt and its intensity scale is 0.05 times that of the other spectra. All spectra were obtained using a CP contact time of 2 ms. Peak assignments under the TMAAI spectra refer to the C atoms indicated on the TMAA molecule to the left of the spectra.

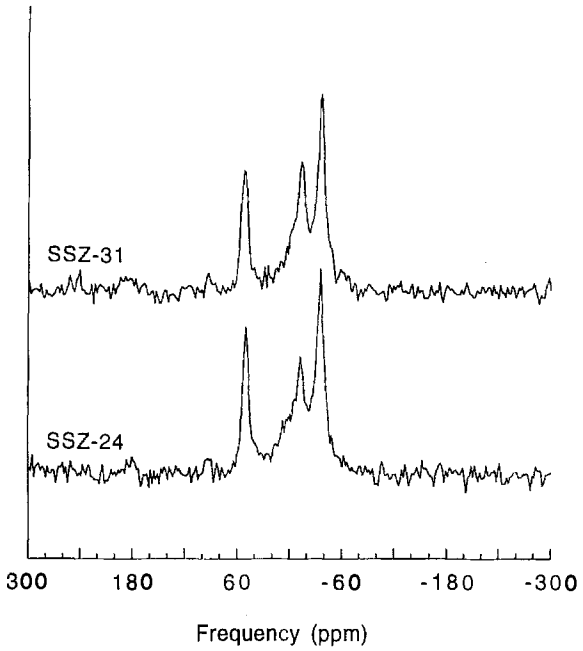

Fig. 9. ^{1}H–^{13}C CP MAS NMR spectra of $TMAA^{+}$ within the SSZ-24 and SSZ-31 lattices.

towards non-zeolitic silicates is not fully understood at this time.

The results of NMR spectroscopy and elemental analysis for SSZ-31 synthesis from Na-TMAA synthesis mixtures are similar to the results reported recently for SSZ-24 synthesis from K-TMAA synthesis mixtures [19]. In both systems, the Si/TMAA ratio in the solids increases during the induction period, and decreases steadily during crystal growth (fig. 6). Also, there is a sharp rise in the pH of the mother liquor during crystal growth in both systems. There is a decrease in the Q^3 to Q^4 ratio during crystal growth in both the Na^{+} (fig. 7a) and K^{+} [19] systems, indicating polymerization of the silicate gel occurs during that time. ^{1}H–^{29}Si CP MAS NMR indicates that there is no cross-polarization between the $TMAA^{+}$ protons and the Si atoms in the amorphous gel during the induction period in either system (fig. 7b). However, there is cross-polarization between the $TMAA^{+}$ protons and the Si atoms in the solids as crystalline zeolite grows in the synthesis gel. This suggests that the $TMAA^{+}$ cations are not within close contact of the silica in the solids (Si–H $\leqslant$ 3.3 Å) until the $TMAA^{+}$ cations are inside the channels of the crystalline zeolite. Changes in the chemical shifts of the peaks in the ^{1}H–^{13}C CP MAS NMR spectra during crystal growth indicate that the structure and mobility of the $TMAA^{+}$ cations change upon incorporation into the SSZ-24 and SSZ-31 lattices (fig. 8). ^{1}H–^{13}C CP MAS NMR also indicates that the structures of $TMAA^{+}$ cations within the SSZ-24 and SSZ-31 channels are similar (fig. 9).

The strong similarities between the observations reported here for SSZ-31 synthesis from synthesis mixtures containing Na^{+} and $TMAA^{+}$ cations and those reported recently for SSZ-24 synthesis from K-TMAA synthesis mixtures [19] suggest that the mechanism for zeolite synthesis is the same in both systems. The first step of the synthesis is the dissolution of the condensed silica forming an alkaline solution rich in low molecular weight silicate anions. Upon further heating, zeolite nucleation occurs as the $TMAA^{+}$ cations interact with the anionic silica in either the gel or solution phase of the synthesis mixture through coulombic and van der Waals attractive forces between the organic cation and the silica. Upon the onset of nucleation, crystallization occurs relatively rapidly as the amorphous gel transforms into crystalline zeolite. The facts that $TMAA^{+}$ is incorporated into the solid products obtained from synthesis mixtures prepared using all of the alkali cations, and that the structure of the $TMAA^{+}$ is similar within the SSZ-24 and SSZ-31 channels, suggest that the alkali cations do not affect the interactions between the $TMAA^{+}$ and the silica, but rather that the alkali cations influence how the silicate gel which contains the organic cations transforms into the crystalline products.

5. Conclusions

Alkali cations play a significant role in the crystallization of zeolites and other silicates from siliceous synthesis mixtures containing $TMAA^{+}$ cations. This study presents a clear example of different zeolite phases crystallizing from siliceous mixtures containing different alkali cations. SSZ-24 crystallizes from K–TMAA synthesis mixtures, and SSZ-31 crystallizes from Na–TMAA synthesis mixtures. This is the first report of the synthesis of SSZ-31 in the presence of $TMAA^{+}$ cations. Unidentified silicates form when Rb^{+} or Cs^{+} are present in the synthesis mixtures, whereas no crystalline material forms from a synthesis mixture prepared without any alkali cations.

The absence of alkali cations in the crystalline products suggests that alkali cations do not serve as structure-directing agents for zeolite synthesis in these systems. Furthermore, it does not appear that the primary role of the alkali cations is to stabilize soluble silicate species in the synthesis mixtures which serve as building blocks for zeolite crystallization. The similar structure of $TMAA^{+}$ cations within the SSZ-24 and SSZ-31 channels indicates that the alkali cations do not strongly influence the interactions between the organic and the silica. The most likely role of the alkali cations is to affect the transformation of the amorphous silicate gels which contain $TMAA^{+}$ cations into crystalline zeolite and other silicate structures.

Acknowledgement

This work was supported by the Director of the Office

of Basic Energy Sciences, Materials Sciences Division, of the US Department of Energy under contract DE-AC03-76SF00098.

References

[1] C.D. Chang and A.T. Bell, Catal. Lett. 8 (1991) 305.
[2] H. Gies and B. Marler, Zeolites 12 (1992) 42.
[3] C.S. Gittleman, A.T. Bell and C.J. Radke, Micropor. Mater. 2 (1994) 145.
[4] C.S. Gittleman, S.S. Lee, A.T. Bell and C.J. Radke, Micropor. Mater. 3 (1995) 511.
[5] S.L. Burkett and M.E. Davis, J. Phys. Chem. 98 (1994) 4647.
[6] S.L. Burkett and M.E. Davis, Chem. Mater. 7 (1995) 920.
[7] R. Szostak, *Molecular Sieves: Principles of Synthesis and Identification* (Van Nostrand Reinhold, New York, 1989) p. 73.
[8] A. Araya and B.M. Lowe, Zeolites 4 (1984) 280.
[9] A. Natsro and L.B. Sand, Zeolites 3 (1983) 57.
[10] A. Erdem and L.B. Sand, J. Catal. 60 (1979) 241.
[11] J.B. Nagy, P. Bodart, H. Collette, J. El Hage-Al Asswad, Z. Gabelica, R. Aiello, A. Nastro and C. Pellegrino, Zeolites 8 (1988) 209.
[12] K. Tu and R. Xu, in: *Zeolites, Synthesis, Structure, Technology and Application*, eds. B. Dryaj, S. Hocevar and S. Pejovnik (Elsevier, Amsterdam, 1985) p. 73.
[13] R.A. Van Nordstrand, D.S. Santilli and S.I. Zones, in: *ACS Symp. Ser.*, Vol. 368, eds. W.H. Frank and T.E. Whyte Jr. (Am. Chem. Soc., Washington, 1988) p. 236.
[14] R. Bialek, W.M. Meier, M. Davis and M.J. Annen, Zeolites 11 (1991) 438.
[15] Y. Nakagawa, US Patent 5271922 (1993).
[16] *Analysis of Geological Samples*, Leeman Applications (Leeman Labs, Lowell, 1984).
[17] D.M. Ginter, A.T. Bell and C.J. Radke, J. Magn. Reson. 81 (1989) 217.
[18] D.A. Torchia, J. Magn. Reson. 30 (1978) 613.
[19] C.S. Gittleman, K. Watanabe, A.T. Bell and C.J. Radke, Micropor. Mater., submitted.
[20] S.I. Zones, T.V. Harris, A. Rainis and D.S. Santilli, US Patent 5,106,801 (1992).
[21] Y. Nakagawa and S.I. Zones, in: *Synthesis of Microporous Materials*, eds. M.L. Occelli and H.E. Robson (Van Nostrand Reinhold, New York, 1992) p. 222.
[22] F. Lefebvre, M. Sacerdote-Peronnet and B.F. Mentzen, Compt. Rend. Acad. Sci. Paris, Ser. 2 316 (1993) 1549.
[23] D.M. Ginter, PhD Thesis, University of California, Berkeley, USA (1991).
[24] C.P. Slichter, *Principles of Magnetic Resonance* (Springer, Berlin, 1980) p. 75.
[25] A.V. McCormick, PhD Thesis, University of California, Berkeley, USA (1987).
[26] W.M. Hendricks, A.T. Bell and C.J. Radke, J. Phys. Chem. 95 (1991) 9513.
[27] E.J.J. Groenen, A.G.T.G. Kortbeek, M. Mackay and O. Sudmeijer, Zeolites 6 (1986) 403.
[28] E.M. Flanigen, J.M. Bennett, R.W. Grose, J.P. Cohen, R.L. Patton, R.M. Kirchner and J.V. Smith, Nature 271 (1978) 512.
[29] J. Depasse and A. Watillon, J. Coll. Interf. Sci. 33 (1970) 431.
[30] R.K. Iler, *The Chemistry of Silica* (Wiley, New York, 1979) p. 666.